

## Characterization of CoNi based catalyst for Water Gas Shift Reaction

Noor Azlina Halim<sup>1</sup>, Noor Shawal Nasri<sup>1</sup>, Ahmad Rahman Songip<sup>2</sup>

<sup>1</sup>Department of Gas Engineering, Faculty of Chemical and Natural Resources Engineering,  
Universiti Teknologi Malaysia, 81310 Skudai, Johor.  
Tel: +607-5535570, Fax: +607- E-mail: noorazlina@utm.my, r-shawal@utm.my

<sup>2</sup>Department of Chemical Engineering, Faculty of Chemical and Natural Resources Engineering,  
Universiti Teknologi Malaysia, 81310 Skudai, Johor.  
Tel: 03-2693302, Fax: +603-26911294, Email: ahmadrs@utmkl.utm.my.

## Abstract

In order to avoid the proton exchange membrane fuel cell (PEMFC) anode (Pt) to be poisonous, the amount of carbon monoxide (CO) in hydrogen stream must be less than 10 ppm. So, water gas shift reaction (WGSR) is applied to purify the hydrogen stream before entering the PEMFC. An emerging use for WGS reaction is on-board hydrogen production for fuel cell vehicles. In WGSR, catalyst plays an important role. The WGSR system in this study used CoNi based (ATR catalyst) as its catalyst. To improve the performance of the catalyst, three different promoters were added to each different sample. They are manganese (Mn), iron (Fe) or chromium (Cr). The main objective of this paper is to study the characterization of X-CoNi/MgO (X= Mn or Fe or Cr) for WGSR. Firstly, each catalyst had to undergo the X-ray Diffraction (XRD) analysis. This analysis is conducted to identify the crystalline phases that were present. Furthermore, Temperature Programmed Reduction (TPR) was used to observe the concentration of reducible species present in the catalyst. From XRD and TPR, all of catalysts were found to be free from NiO and CoO that contribute to sintering and coke formation. TPR also represents the activity of catalysts were related with reduction temperature. The activity of catalysts was increased when temperature reduction of catalyst was increased. From the results of experiment, FeO-NiOCoO/MgO with 3wt% has a high activity compared to others.

**Keywords:** Water gas shift reaction, Fuel Cells, PEMFC, TPR and XRD

## Introduction

In automotive application, proton exchange membrane fuel cell (PEMFC) system has received much attention as a compact generator. The system has an advantage from the viewpoint of high energy density and compactness see [1]. In this system, hydrogen is used as a fuel; it is produced from synthesis gas (syngas) by steam reforming (SR) see [2], partial oxidation (POX) see [3, 4] or autothermal reforming (ATR) of hydrocarbon see [5, 6]. The problem

is that the syngas (H<sub>2</sub> & CO) contains CO at the level of 1-10%, which adsorbs irreversibly on the Pt electrode of PEMFC and hinders the electrochemical reaction see [1]. Therefore, CO must be removed from the syngas to less than 10 ppm before feeding the gas mixture to Pt electrode. So, purified H<sub>2</sub> is then produced by allowing syngas to react with steam according to the following exothermic water gas shift reaction (WGSR) see [7, 8]:



The equilibrium conversion of CO is dependent largely on the reaction temperature, since WGSR is an exothermic reaction, lower temperature is favored for higher CO removal see [1, 9]. On the other hand, from the viewpoint of kinetics, the reactant gases are not active enough to reach the chemical equilibrium at low temperature and high temperature is needed to achieve rates of industrial application. Therefore, there exists an optimum temperature for WGSR; in general the optimum temperature is between 200-280°C see [1].

According to Meyers *et al.* see [10], the conventional WGSR process used two different catalysts, designed for two distinctive temperature regimes for stationary systems. They were Fe/Cr catalyst for high temperature (HT) condition and Cu/ZnO catalyst for low temperature (LT) condition. Both of them have lots of weaknesses. Firstly, they required activation by pre-reduction *in situ*. Next, the pyrophoric (loses activity) were happened when exposed to air or steam. In addition, certain range of temperature condition requires different type of catalyst; for example the operating temperature of HT catalyst is 300°C and below and the LT catalyst temperature range is less than 250°C. Finally, the catalyst must be separated during system shutdown.

The main objective of this study is to develop WGSR system using ATR catalyst (NiOCoO/MgO) see [11] at high temperature. Some of promoters (FeO or CrO or MnO) were added to improve the catalyst for WGSR system with high catalytic activity and high stability.

## Experimental

### Catalysts preparation

In this study, magnesium oxide (MgO) has been chosen as a support and magnesium nitrate hexahydrate ( $\text{Mg}(\text{NO}_3)_2 \cdot 6\text{H}_2\text{O}$ ) has been selected as a precursor. Firstly, precursor of support is dissolved in the distilled water, then dried overnight at  $110^\circ\text{C}$  and calcined at  $800^\circ\text{C}$  for 8 hours see [4, 5]. After that, crushed and sieved to 100 meshes.

The catalysts were prepared by co-impregnating the support (MgO) with mixed aqueous solutions of  $\text{Co}(\text{NO}_3)_2 \cdot 6\text{H}_2\text{O}$ ,  $\text{Ni}(\text{NO}_3)_2 \cdot 6\text{H}_2\text{O}$  and  $\text{X}_s$  ( $\text{X}_s = \text{Mn}(\text{NO}_3)_2 \cdot 4\text{H}_2\text{O}$  or  $\text{Fe}(\text{NO}_3)_3 \cdot 9\text{H}_2\text{O}$ ). The required amount of nickel nitrate, cobalt nitrate and  $\text{X}_s$  were weighed and dissolved in distilled water, subsequently the support was added. After gentle stirring for 3 hours, the slurry was heated to  $50\text{--}70^\circ\text{C}$  until dry, followed by overnight drying at  $110^\circ\text{C}$  and calcined at  $800^\circ\text{C}$  for 8 hours. All the catalysts were then crushed and sieved to 100 meshes.

### Methods of characterization

Temperature-programmed reduction (TPR) experiments were performed on Thermo Finnigan TPDRO 1100 instrument. The sample of catalyst was first pretreated in a flow of  $\text{N}_2$  from 100 to  $750^\circ\text{C}$ , with a temperature gradient of  $25^\circ\text{C}/\text{min}$  and flow of 20 ml/min. The pretreatment was held for 60 minutes after the temperature reached at  $750^\circ\text{C}$ . The reduction gas used was 5%  $\text{H}_2$  in  $\text{N}_2$ . The experiments were run in the range of  $100\text{--}900^\circ\text{C}$  with approximately 45 mg sample, a temperature gradient of  $20^\circ\text{C}/\text{min}$ , flow of 35 ml/min and the run was held for 15 minutes.

The crystalline phase of the catalysts was determined by powder X-Ray diffraction (XRD) technique on a Bruker XRD D8 Advance diffractometer using  $\text{Cu K}\alpha$  radiation. The diffraction data were recorded for  $2\theta$  angles between  $10^\circ$  to  $80^\circ$ , with a resolution of  $0.05^\circ$ .

### Evaluation of catalytic activity

Before running the activity testing, the preheating of reactor was executed at  $500^\circ\text{C}$  under a 100 ml/min-nitrogen stream for an hour to activate the catalyst. The feed was a mixture of carbon monoxide and steam whereas nitrogen is the carrier gas. The catalytic activity was examined using a quartz reactor at atmospheric pressure in the temperature range from  $400\text{--}800^\circ\text{C}$  using 0.5g of catalysts. The gas composition after the reaction was analyzed by on-line gas chromatography with a thermal conductivity detector.

## Result and Discussion

### Catalyst characterization

The physical properties of catalysts have been studied using the TPR and XRD analysis. TPR was used to study the concentration of reducible species present in the

catalyst and XRD to analyze the crystalline structure in the catalyst.

### XRD profile

#### $\text{FeO-NiOCoO/MgO}$

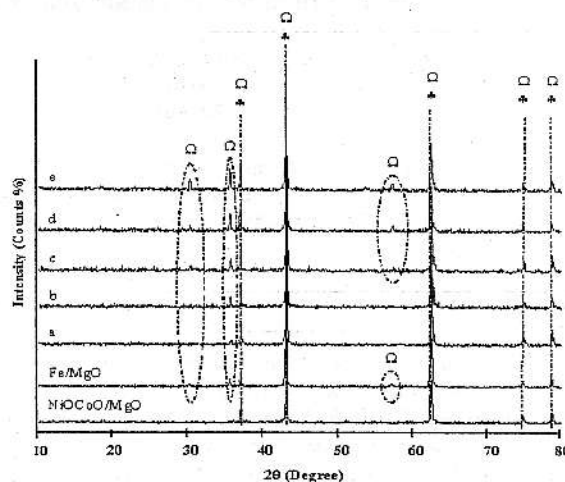


Figure 1: XRD patterns of various weights loading of iron: (a) 1.5wt%  $\text{FeO-NiOCoO/MgO}$ ; (b) 3wt%  $\text{FeO-NiOCoO/MgO}$ ; (c) 5wt%  $\text{FeO-NiOCoO/MgO}$ ; (d) 7wt%  $\text{FeO-NiOCoO/MgO}$ ; (e) 10wt%  $\text{FeO-NiOCoO/MgO}$ ; ( $\star$ )  $\text{NiOCoO/MgO}$ ; ( $\square$ )  $\text{MgFe}_2\text{O}_4$

Figure 1 represents the XRD patterns of  $\text{FeO-NiOCoO/MgO}$  with various weights loading of iron and  $\text{FeO/MgO}$  and  $\text{NiOCoO/MgO}$  solid solution as a reference. The peaks of  $\text{NiOCoO/MgO}$  see [11] and  $\text{MgFe}_2\text{O}_4$  overlapped each other at  $37^\circ$ ,  $43^\circ$ ,  $62.3^\circ$ ,  $74.7^\circ$  and  $78.7^\circ$  of  $2\theta$ . The  $\text{MgFe}_2\text{O}_4$  peaks also existed at  $30.1^\circ$ ,  $62.3^\circ$  and  $78.7^\circ$  of  $2\theta$ . These peaks were similar with Bond *et al.* [12]. The overlapping is due to same distance between atoms species and the same cubic structure.

The XRD patterns for 1.5wt% and 3wt% Fe is quite similar with  $\text{NiOCoO/MgO}$  solid solution. It is maybe the iron oxide was dispersed highly in MgO support or due to small amounts of iron were added into the catalyst. The clear peaks of  $\text{MgFe}_2\text{O}_4$  were observed at 5wt%, 7wt% and 10wt% Fe. The peaks become stronger when more amounts of iron were added. It is shown in the TPR profile when the present of iron oxide facilitates the reduction of  $\text{NiOCoO/MgO}$  solid solution from  $900^\circ\text{C}$  to around the range of  $620^\circ\text{C}$  to  $700^\circ\text{C}$ .

This figure also shows these catalysts were free from NiO or CoO that causes a sintering and coking. This is approved with the TPR profile of  $\text{FeO-NiOCoO/MgO}$  when no peak either NiO or CoO were present.

## CrO-NiOCoO/MgO

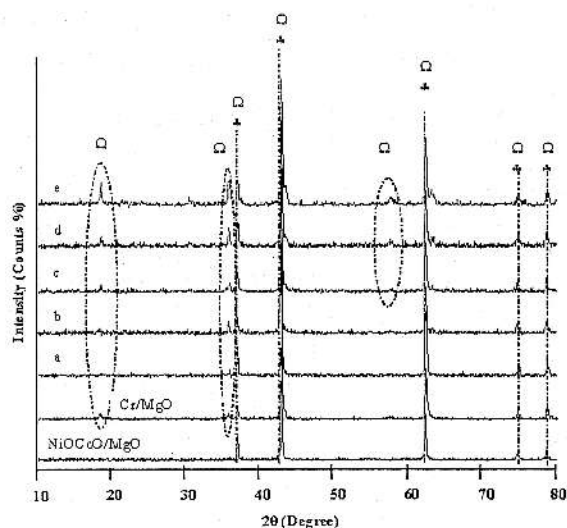


Figure 2: XRD patterns of various weights loading of chromium: (a) 1.5wt%CrO-NiOCoO/Mg; (b) 3wt%CrO-NiOCoO/Mg; (c) 5wt%CrO-NiOCoO/MgO; (d) 7wt%CrO-NiOCoO/MgO; (e) 10wt%CrO-NiOCoO/MgO: (♣) NiOCoO/MgO; (Ω)  $\text{CoCr}_2\text{O}_4$ ,  $\text{MgCr}_2\text{O}_4$  and  $\text{NiCr}_2\text{O}_4$ .

The XRD pattern of CrO-NiOCoO/MgO with various weights loading of Cr is shown in Figure 2. This figure also includes the profiles of CrO/MgO and NiOCoO/MgO solid solution as references.

The peaks of NiOCoO/MgO solid solution,  $\text{CoCr}_2\text{O}_4$ ,  $\text{MgCr}_2\text{O}_4$  and  $\text{NiCr}_2\text{O}_4$  were overlapped at  $2\theta = 37^\circ$ ,  $43^\circ$ ,  $62.3^\circ$ ,  $74.7^\circ$  and  $78.7^\circ$ . The result of  $\text{MgCr}_2\text{O}_4$  peaks is similar with El-Molla see [13] when  $\text{Cr}_2\text{O}_3/\text{MgO}$  samples were calcined at  $700^\circ\text{C}$ .

Inspection of this figure revealed that intensity of  $\text{CoCr}_2\text{O}_4$ ,  $\text{MgCr}_2\text{O}_4$  and  $\text{NiCr}_2\text{O}_4$  increase when amount of chromium was increased. It was happened according to the rest amount of  $\text{Cr}_2\text{O}_3$  can interact with Co, Ni and MgO to form other solid solution see [13].

## MnO-NiOCoO/MgO

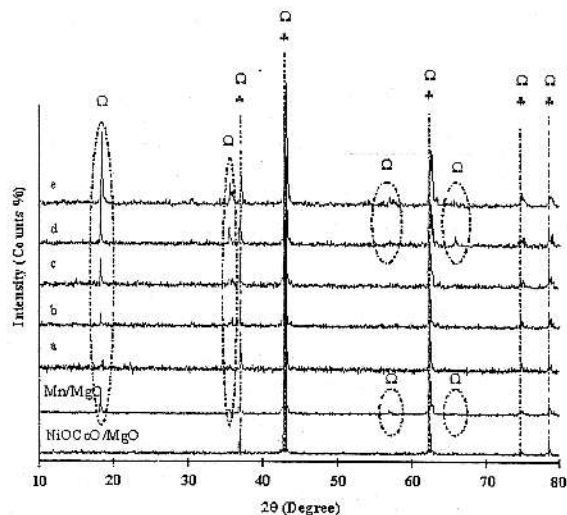


Figure 3: XRD patterns of the various weights loading of manganese: (a) 1.5wt%MnO-NiOCoO/Mg; (b) 3wt%MnO-NiOCoO/MgO; (c) 5wt%MnO-NiOCoO/MgO; (d) 7wt%MnO-NiOCoO/MgO; (e) 10wt%MnO-NiOCoO/MgO: (♣) NiOCoO/MgO; (Ω)  $\text{Mg}_6\text{MnO}_8$ .

Figure 3 shows the XRD profile for the various weights loading of manganese in MnO-NiOCoO/MgO. As a reference, the XRD pattern of MnO/MgO and NiO-CoO/MgO solid solution are also include in this figure.

This figure shows that the peaks of NiOCoO/MgO and  $\text{Mg}_6\text{MnO}_8$  were overlapped each other at  $37^\circ$ ,  $43^\circ$ ,  $62.3^\circ$ ,  $74.7^\circ$  and  $78.7^\circ$  of  $2\theta$ , whereas a single peak of  $\text{Mg}_6\text{MnO}_8$  were detected at  $18^\circ$  and  $37^\circ$  of  $2\theta$ . The Peak of  $\text{Mg}_6\text{MnO}_8$  was similar with Chen *et al.* see [14, 15].

From this figure, when manganese was added in NiO-CoO/MgO the structure of solid solution was modified to form other structure.

## TPR profile

## FeO-NiOCoO/MgO

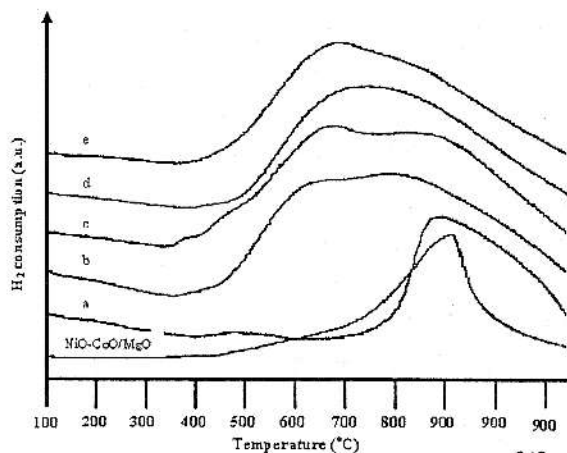


Figure 4: TPR profile of various weights loading of iron: (a) 1.5wt%FeO-NiOCoO/MgO; (b) 3wt%FeO-NiOCoO/MgO; (c) 5wt%FeO-NiOCoO/MgO; (d) 7wt%FeO-NiOCoO/MgO; (e) 10wt%FeO-NiOCoO/MgO

Figure 4 represents the TPR profile for FeO-NiOCoO/MgO with various weights loading of iron and NiOCoO/MgO. This figure shown the profile of FeO-NiOCoO/MgO has three patterns. First pattern represented with 1.5wt%Fe where it is profile same as NiOCoO/MgO. It has a strong peak at 900 °C. For 3wt%Fe, it has a similar pattern with 5wt%Fe where two peaks were detected at 600°C and around 800-900°C. Around 650°C and 750°C a similar pattern were observed for 7wt%Fe and 10wt%Fe.

According to Tutuk see [11], a peak at 900°C is a NiOCoO/MgO solid solution where it is has a strong interaction with support. For 1.5wt%Fe, a peak at 900°C still detected may be the amounts of iron not necessary distract the structure of NiOCoO/MgO solid solution.

Once the amount of iron was added at 3wt% and above, the structure of NiOCoO/MgO solid solution has been changed. For 3wt% and 5wt%Fe, the peak at 900°C still detected but the intensity of peaks too low. The intensity of peak at 600°C also increased when amount of iron was increased. These peaks may be assigned for reduction from  $\text{MgFe}_2\text{O}_4$  that has been detected in XRD analysis.

Figure 4 also shows that 7wt% and 10wt%Fe have different with 1.5wt%, 3wt% and 5wt%. At 7wt% and 10wt%Fe, the compound in this solution was highly dispersed and maybe existed a special solution that consist  $\text{MgFe}_2\text{O}_4$ . This result similar with Bond *et al.* see [12] where they highlighted that the reduction of  $\text{MgFe}_2\text{O}_4$  is capable to form the solid solution  $\text{Fe}_x\text{Mg}_{1-x}\text{O}$ , thereby stabilizing some of the iron as  $\text{Fe}^{2+}$  and leading to the formation of very finely-divided iron.

The intensity of 10wt%Fe is higher than 7wt% where the amount of  $\text{MgFe}_2\text{O}_4$  in the solution is increased. The NiOCoO/MgO solid solution maybe exist in both of catalysts but it exist in too small amount, so difficult to analyze by TPR.

#### CrO-NiOCoO/MgO

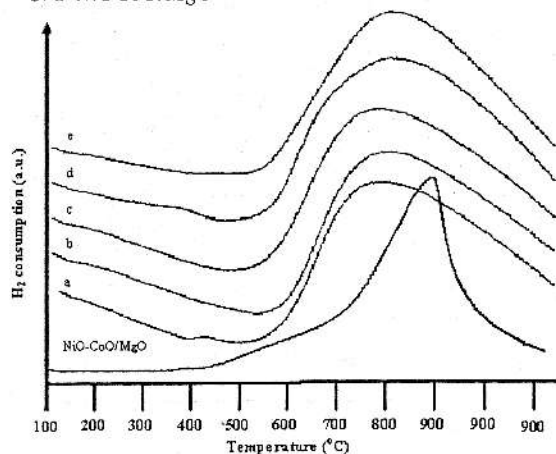


Figure 5: TPR profile of various weights loading of chromium: (a) 1.5wt%CrO-NiOCoO/Mg; (b) 3wt%CrO-NiOCoO/Mg; (c) 5wt%CrO-NiOCoO/MgO; (d) 7wt%CrO-NiOCoO/MgO; (e) 10wt%CrO-NiOCoO/MgO.

The TPR profile for CrO-NiOCoO/MgO with various weights loading of chromium and NiOCoO/MgO are shown in Figure 5. Compared with Figure 4 and Figure 6, this figure gives very smooth and similar patterns.

From this figure, all of peaks only seemed at 750°C. It is may be the CrO-NiOCoO/MgO existed as an ideal solution. The compounds in this catalyst highly dispersed due to strong metal-support interaction. This agreed with XRD where  $\text{CoCr}_2\text{O}_4$ ,  $\text{MgCr}_2\text{O}_4$  and  $\text{NiCr}_2\text{O}_4$  were detected in this analysis.

Besides that, this figure also illustrated that no peak of CoO and NiO free as an agent for sintering and coke formation.

#### MnO-NiOCoO/MgO

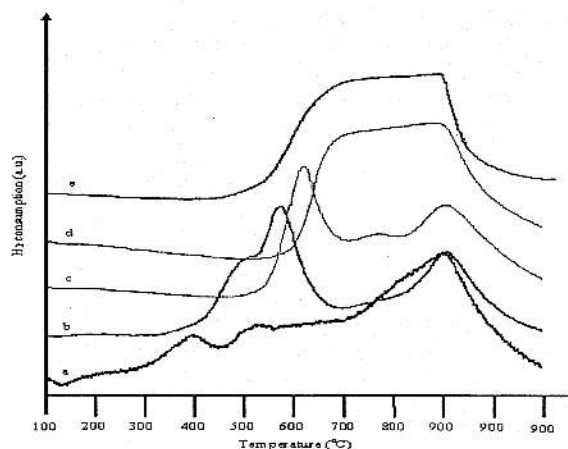


Figure 6: TPR profile of the various weights loading of manganese: (a) 1.5wt%MnO-NiOCoO/Mg; (b) 3wt%MnO-NiOCoO/MgO; (c) 5wt%MnO-NiOCoO/MgO; (d) 7wt%MnO-NiOCoO/MgO; (e) 10wt%MnO-NiOCoO/MgO

Figure 6 shows the TPR profile MnO-NiOCoO/MgO with various weights loading of manganese. From this figure, every catalyst has a peak at 900°C. That peak assigned as NiOCoO/MgO solid solution by Tutuk see [11].

Figures 6 shown two peaks in 1.5wt%, 3wt% and 5wt% profile, these peaks represent two-step reduction. The two reduction peaks on the profile correspond to subsequent reduction of  $\text{MnO}_2$  to  $\text{Mn}_2\text{O}_3/\text{Mn}_3\text{O}_4$  and MnO see [14] but these species cannot detect in XRD measurement maybe it was presented in small amount. From this figure, manganese oxide was not highly dispersed when the reduction peaks of manganese oxide where detected in TPR profile.



According to Chen *et al.* see [14], the 10%Mn/MgO catalyst is irreducible before 600°C due to the formation of the complex oxide ( $\text{Mg}_6\text{MnO}_8$ ). In this case, broad peaks were present at 650°C; it is maybe the structure of  $\text{Mg}_6\text{MnO}_8$  was presented. This species were agreed with XRD measurement, whereas at 1.5wt%, 3wt% and 5wt% this species not detected in TPR profile maybe  $\text{Mg}_6\text{MnO}_8$  present in small amount.

Figure 6 also illustrated that no peak of CoO and NiO free as an agent for sintering and coke formation.

#### Effect of Catalysts Composition

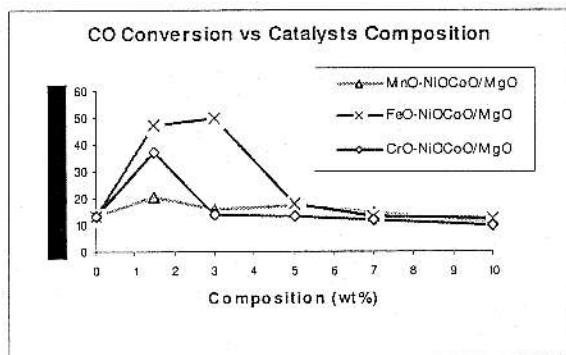


Figure 7: Effect Of Catalysts Composition at 400°C and  $\text{H}_2\text{O}/\text{CO}=2$ .

Figure 7 shows the effect of 1.5wt%, 3wt%, 5wt%, 7wt% and 10wt% of promoters (MnO or FeO or CrO) added in  $\text{NiOCoO}/\text{MgO}$  solid solution (ATR catalyst). This figure was highlighted the activity of WGS was decreased when amount of promoter was increased. In  $\text{FeO-NiOCoO}/\text{MgO}$ , the activity was drastically dropped from 50% to less than 20% after 3wt% of FeO was added. However,  $\text{MnO-NiOCoO}/\text{MgO}$  and  $\text{CrO-NiOCoO}/\text{MgO}$  also have the same scenario and most terrible when their performance only retain at 1.5wt% and constantly dropped after that. They are also not attracted due to their performance not achieved as high as  $\text{FeO-NiOCoO}/\text{MgO}$ . The highest CO conversion  $\text{CrO-NiOCoO}/\text{MgO}$  was achieved is less than 40% and the worst is  $\text{MnO-NiOCoO}/\text{MgO}$  with 20%. From TPR observation the activity of catalysts were related with reduction temperature. The activity of catalysts was increased when temperature reduction of catalyst increased. So, from this effect 3wt% $\text{FeO-NiOCoO}/\text{MgO}$  is the best and will continue to investigate in other effects like temperature reaction and  $\text{H}_2\text{O}/\text{CO}$  ratio.

#### Conclusion

From XRD and TPR analysis, all of catalysts were free from NiO and CoO peaks that contribute to sintering and coke formation. From this study 3wt% $\text{FeO-NiOCoO}/\text{MgO}$  gave the best catalyst compared to others

where the CO conversion almost 50%. So, only 3wt% $\text{FeO-NiOCoO}/\text{MgO}$  has been chosen to continue this study using other parameters like temperature and  $\text{H}_2\text{O}/\text{CO}$  ratio.

#### Acknowledgements

The authors would like to thank the Malaysian Ministry of Science, Technology & Innovation (MOSTI) for sponsoring this work under project IRPA 03-02-06-0033 PR0023/11-04.

#### References

- [1] Tanaka, Y., Utaka, T., Kikuchi, R., Sazaki, K. and Eguchi, K. (2003). Water gas shift reaction over Cu-based mixed oxides for CO removal from the reformed fuels. *Applied Catalysis A: General* **242**, 287-295.
- [2] Hegarty, M. E. S., O'Connor, A. M. and Ross, J. R. H. (1998). "Syngas production from natural gas using  $\text{ZrO}_2$ -supported metals". *Catalysis Today* **42**, 225-232.
- [3] Lago, R., Bini, G., Pena, M. A. and Fierro, J. L. G. (1997). Partial oxidation of methane to synthesis gas using  $\text{LnCoO}_3$  perovskites as catalyst precursors. *Journal of Catalysis* **167**, 198-209.
- [4] Wang, H.Y. and Ruckenstein, E. (2001). Partial oxidation of  $\text{CH}_4$  to synthesis gas over Alkaline Earth Metal oxide supported Co catalysts. *Journal of Catalysis* **199**: 309-317.
- [5] Ma, L. and Trimm, D.L. (1996). Alternative catalyst bed configurations for the autothermic conversion of methane to hydrogen. *Applied Catalysis A: General* **138**, 267-273.
- [6] Takeguchi, T., Furukawa, S. N., Inoue, M. and Eguchi, K. (2003). Autothermal Reforming of Methane over Ni Catalysts Supported over  $\text{CaO-CeO}_2\text{-ZrO}_2$  Solid Solution. *Applied Catalysis A: General* **240**: 633-642.
- [7] Twigg, M. V. (1989). Catalyst Handbook. Second edition. England. 293-308.
- [8] Costa, J. L. R., Marchetti, G. S. and Rangel, M. D. C. (2002). A thorium-doped catalyst for the high Temperature Shift Reaction. *Catalysis Today* **77**, 205-213.
- [9] Laine, R. M. and Crawford E. J. (1988). Homogeneous Catalysis of the water gas shift reaction. *Journal of Molecular Catalysis* **44**, 357-387.
- [10] Meyers, D.J., Krebs, J.F., Krause, T.R. and Krumpelt, M. (2000). In: Annual progress report, US DOE, Energy

- Efficiency and Renewable Energy, Office of Transportation Technologies. "Alternative Water Gas Shift Catalyst Development." 70-74.
- [11] Tutuk, D. K. (2004). Autothermal reforming and partial oxidation of methane for hydrogen production using NiO-CoO/MgO catalyst. Master Thesis.
- [12] Bond, G., Molloy, K. C. and Stone, F. S. (1997). Reduction of MgO-supported iron oxide: Formation and Characterization of Fe/MgO Catalysts. *Solid State Ionics*. **101-103**: 697-705.
- [13] El-Molla, S. A. (2005). Surface and Catalytic Properties of Cr<sub>2</sub>O<sub>3</sub>/MgO System Doped With Manganese and Cobalt Oxides. *Applied Catalysis A: General*. **280**: 189-197.
- [14] Chen, A., Xu, H., Yue, Y., Hua, W., Shen, W. and Gao, Z. (2003). Supported Effect in Hydrogenation of Methyl Benzoate Over supported Manganese Oxide Catalysts. *Journal of Molecular Catalysis A: Chemical*. **203**: 299-306.
- [15] Chen, A., Xu, H., Yue, Y., Hua, W., Shen, W. and Gao, Z. (2003). Hydrogenation of Methyl Benzoate Over supported Manganese Oxide Catalysts Prepared from Mg/Mn/Al Hydrate-like Compounds. *Applied Catalysis A: General*. **274**: 101-109.